The Astrophysical Journal Supplement Series, 154:453–457, 2004 September

MID-INFRARED SPECTRA OF DUST DEBRIS AROUND MAIN-SEQUENCE STARS[1]

M. Jura,[2] C. H. Chen,[3] E. Furlan,[4] J. Green,[5] B. Sargent,[5] W. J. Forrest,[5] D. M. Watson,[5] D. J. Barry,[4] P. Hall,[4] T. L. Herter,[4] J. R. Houck,[4] G. C. Sloan,[4] K. Uchida,[4] P. D'Alessio,[6] B. R. Brandl,[7] L. D. Keller,[8] F. Kemper,[2,9] P. Morris,[10] J. Najita,[11] N. Calvet,[12] L. Hartmann,[12] and P. C. Myers[12]

Received 2004 March 26; accepted 2004 May 27

ABSTRACT

We report spectra obtained with the *Spitzer* Space Telescope in the $\lambda = 14-35$ μm range of 19 nearby main-sequence stars with infrared excesses. The six stars with strong dust emission show no recognizable spectral features, suggesting that the bulk of the emitting particles have diameters larger than 10 μm. If the observed dust results from collisional grinding of larger solids, we infer minimum masses of the parent body population between 0.004 and 0.06 $M_{\oplus}$. We estimate grain production rates of $\sim 10^{10}$ g s^{-1} around λ Boo and HR 1570; selective accretion of this matter may help explain their peculiar surface abundances. There appear to be inner truncations in the dust clouds at 48, 11, 52, and 54 AU around HR 333, HR 506, HR 1082, and HR 3927, respectively.

Subject headings: circumstellar matter — infrared: stars

1. INTRODUCTION

The discovery with *IRAS* of a large infrared excess around Vega (Aumann et al. 1984) initiated the detailed study of other planetary systems. We can now use the dust emission from main-sequence stars to constrain models for the origin and evolution of these environments (Lagrange et al. 2000; Zuckerman 2001) with the long-term goal of developing a more comprehensive understanding of the formation and evolution of planets and related minor bodies. Most previous studies of the dust around main-sequence stars have been restricted to using broadband infrared fluxes (e.g., Habing et al. 2001; Spangler et al. 2001). Here we report measurements with the Infrared Spectrograph (IRS; Houck et al. 2004)[13] on the *Spitzer Space Telescope* (Werner et al. 2004) of 19 main-sequence stars.

2. OBSERVATIONS

We obtained spectra of main-sequence stars with previously reported *IRAS* excesses with both the Short-Low (5.2–14.5 μm) and Long-Low (14.0–38.0 μm; $\lambda/\Delta\lambda \sim 90$) modules on the IRS. Table 1 lists the six targets in our sample with strong infrared excesses. We did not detect a substantial excess around 13 other stars. An example of a star without a strong excess is HR 4732; its spectrum (from *Spitzer* AOR 0003579392) is shown in Figure 1 (Plate 1). The other stars without strong excesses are HD 16157 (AOR 0003554560), HD 221354 (AOR 0003565842), HR 818 (AOR 0003554816), HR 1338 (AOR 0003555584), HR 2015 (AOR 0003556608), HR 3220 (AOR 0003557888), HR 3862 (AOR 0003558400), HR 5447 (AOR 0003560192), HR 8085 (AOR 0003564544), HR 8549 (AOR 0003588608), HR 8799 (AOR 0003565568), and Ross 128 (AOR 0003559168).

In order to avoid time-consuming peak-up on our relatively bright targets with accurately known positions, we operated the observatory in IRS spectral mapping mode where a 2×3 raster (spatial x dispersion) centered on the star is performed. The slit positions were separated by half of the slit width in the dispersion direction and by a third of the slit length in the spatial direction.

We carried out the bulk of the reduction and analysis of our spectra with the IRS team's SMART program (Higdon 2004). We started with intermediate products from the *Spitzer* IRS data reduction pipeline that lacked only stray light and flat-fielding corrections. We extracted point-source spectra for each nod position using a uniformly weighted column profile for which the variable width scales with the width of the instrumental point-spread function. We also made similar spectral extractions for observations of our photometric standard star, α Lac (A1 V). Then we divided each target spectrum, nod position by nod position, by the spectrum of the standard star, multiplied the quotient by the appropriate template spectrum (Cohen et al. 2003), and averaged the resulting spectra from corresponding nod positions. We plot the resulting spectra of our targets with IR excesses in Figure 1. Based on comparisons of IRS spectra of nonvariable calibration sources to ground-based, *IRAS*, and *Spitzer* IRAC flux densities, we estimate that the absolute spectrophotometric accuracy of these spectra is 10% (1 σ). It is important to distinguish this absolute photometric accuracy, which describes the vertical positions of the spectra on our plots relative to

[1] Based on observations with the NASA *Spitzer Space Telescope*, which is operated by the California Institute of Technology for NASA.

[2] Department of Physics and Astronomy, University of California, Los Angeles, CA 90095-1562.
[3] Jet Propulsion Laboratory, California Institute of Technology, Pasadena, CA 91109.
[4] Department of Astronomy, Cornell University, Ithaca, NY 14853-6801.
[5] Department of Physics and Astronomy, University of Rochester, Rochester, NY 14627-0171.
[6] Centro de Radioastronomia y Astrofisica, UNAM, 58089 Morelia, Michoacan, Mexico.
[7] Sterrewacht Leiden, 2300 RA Leiden, Netherlands.
[8] Department of Physics, Ithaca College, Ithaca, NY 14850.
[9] *Spitzer* Fellow.
[10] *Spitzer* Science Center, California Institute of Technology, Pasadena, CA 91125.
[11] National Optical Astronomy Observatory, Tucson, AZ 85726-6732.
[12] Harvard Smithsonian Center for Astrophysics, Cambridge, MA 02138.

[13] The IRS was a collaborative venture between Cornell University and the Ball Aerospace Corporation, funded by NASA through the Jet Propulsion Laboratory and the Ames Research Center.

TABLE 1
STARS WITH EXCESSES IN THE IRS DATA

Star	Spectral Type	D (pc)	L_* ($L_\odot$)	t_* (Gyr)	K_2	L_{30}/L_* (10^{-4})	T_{ex} (K)	M_{PB} ($M_\oplus$)	t(exp) (s)	*Spitzer* AOR Key[a]
HR 333.....	A3 V	83	34	0.1	0.16	1	97	0.03	24	0003553536
HR 506.....	F9 V	17	1.5	0.3[b]	0.15	0.9	94	0.004	24	0003553792
HR 1082.....	A3 IV/V	74	12	0.1[b]	0.15	2	72	0.02	24	0003555328
HR 1570.....	A0 V	37	15	0.1[c]	0.14	0.4	88	0.005	24	0003555840
HR 3927.....	A0 V	98	44	0.1	0.21	1	98	0.06	24	0003558656
λ Boo	A0 V	30	15	0.2[c]	0.21	0.4	114	0.01	24	0003559936

[a] The *Spitzer* AOR data file identification number.
[b] Zuckerman & Song (2004).
[c] Heiter et al. (2002). In this table, K_2 (10^{13} Jy Hz) is defined in eq. (1).

the flux density scale, from the point-to-point fluctuation in the spectra, which is a measure of the precision of our spectral feature strengths and therefore of our ability to identify spectral features and compare them to our models. In general, the accuracy of our spectral feature identifications and feature strengths is limited by the point-to-point scatter (currently much larger than the system noise in bright objects) that is visible in the spectra. Therefore, almost all features that significantly exceed the fluctuations, and are wider than the two-pixel IRS spectral resolution element, are significant. The lack of spectral features that we refer to in this paper is based on this criterion.

3. INTERPRETATION AND ANALYSIS

To interpret the data for the infrared excess, we need luminosities, L_*, and ages, t_*, of the stars. We take distances, D_*, from *Hipparcos*, apparent magnitudes from the Yale Bright Star Catalog, assume no interstellar reddening, and use the bolometric corrections given by Flower (1996) to infer the total luminosities. For four stars, we adopt published estimated ages. For HR 506, the age is highly uncertain since Zuckerman & Song (2004) and Decin et al. (2000, 2003) estimate 0.3 and 3.0 Gyr, respectively. In view of the recently measured lithium abundance of 2.6 on the usual 12 point logarithmic scale (Israelian et al. 2004), we adopt the younger age. For HR 333 and HR 3927, we assume ages of 0.1 Gyr, representative of dusty main-sequence A-type stars (Song et al. 2001).

3.1. *Grain Size*

The dust continua for $\lambda > 20$ μm show no spectral features. If the particles are spheres of diameter a, then any spectral features that might be present are weakened if $a > \lambda/\pi$ (e.g., Spitzer 1978; Wolf & Hillenbrand 2003). Our data thus suggest that the diameter of the grains is larger than 10 μm, as predicted by models such as those of Krivov et al. (2000) and found for the particles that produce the zodiacal light in the solar system (Fixsen & Dwek 2002).

3.2. *Spatial Distribution and Dynamics*

A standard model of dust debris systems assumes that collisions among a population of large, unseen parent bodies produces smaller, detectable dust particles (Lagrange et al. 2000; Zuckerman 2001). Some of the best-studied systems such as HR 4796A exhibit a well-defined ring of material (Schneider et al. 1999). Very approximately, for circumstellar envelopes with $L_{30}/L_* > 10^{-4}$ (where L_{30} is the characteristic luminosity of the infrared excess in the 30 μm spectral window, or νL_ν at 30 μm), particle-particle collisions typically are the most important grain destruction mechanism (e.g., Krivov et al. 2000; Wyatt & Dent 2002). In these relatively dusty environments, the grains do not migrate far before they are fragmented into sufficiently small pieces that are driven out of the system by radiation pressure. Thus, the spatial distribution of the dust reproduces the spatial distribution of the parent bodies, which might be determined by the history of planet formation in the system. In contrast, in less dusty envelopes with $L_{30}/L_* < 10^{-4}$, mutual collisions are not so important, and the grains spiral inward under the Poynting-Robertson drag. In such models, the spatial distribution of the grains need not reproduce that of the parent bodies.

Motivated by these models of dust debris, we consider two possible fits to the reduced data. First, we fitted the spectra by a function of the form

$$F_\nu = K_1\nu^2 + K_2\nu^{-1}, \quad (1)$$

where K_1 and K_2 are constants. The first term in equation (1) describes the photospheric emission, while the second term represents the infrared excess. We show in Figure 1 the comparison of our best fits with the data, and we list in Table 1 our values for K_2 and L_{30}/L_*, where L_{30} is $4\pi D_*^2 K_2$. Equation (1) fits the spectra for the two stars with the lowest values of L_{30}/L_*, HR 1570 and λ Boo. However, the infrared excesses of four stars require another model, since fits using equation (1) either underestimate the observed photospheric fluxes measured at $\lambda \leq 12$ μm (HR 333 and HR 3927) or the measured *IRAS* and/or *ISO* fluxes (Decin et al. 2000) at $\lambda = 60$ μm (HR 506 and HR 1082).

Our second method to model the infrared excess is to fit a single temperature to the dust particles so that the total flux is fitted with a function of the form

$$F_\nu = C_1\nu^2 + C_2 B_\nu(T_{ex}), \quad (2)$$

where B_ν is the Planck function. In principle, C_1 must equal K_1, but the absolute level of our spectra is somewhat uncertain because of imprecise calibration. As can be seen in Figure 1 (Plate 1), we can fit our infrared spectra adequately with equation (2) with the values of T_{ex} given in Table 1 ranging from 72 to 114 K.

The spectral energy distribution of the infrared excess can test the models. If the Poynting-Robertson drag dominates, the spectrum varies as ν^{-1} (e.g., Buitrago & Mediavilla 1985), the dust is smeared over a wide range of radii, and equation (1) should fit the data. In contrast, in a model where collisions limit the lifetime of the particles, then inward drift is not as important and the dust is more concentrated near its birthplace. In environments with $L_{30}/L_* > 10^{-4}$, there might be a dust ring or at least a well-defined inner hole to the dust distribution, which achieves a characteristic maximum temperature. Within the limited IRS spectral range, equation (2) can fit the data. Inner dust truncations might be the result of the formation of low-mass companions that might be planets (Kenyon & Bromley 2002), but other models can produce rings as well (Takeuchi & Artymowicz 2001). Also, since $T_{\rm ex}$ is near 100 K, if water ice is an important constituent of the material, there may be substantial grain destruction by sublimation that contributes to the observed deficiency of warm grains (Jura et al. 1998).

We now estimate some parameters for the circumstellar dust. We assume that the particles radiate like blackbodies so that particles at temperature T lie at distance D from the star,

$$D = \left(\frac{L_*}{16\pi T^4 \sigma_{\rm SB}}\right)^{1/2}. \quad (3)$$

For the two stars where the spectra can be fitted by equation (1), there is no constraint on the maximum temperature and thus no evidence of any inner truncation in the dust distribution. There are four stars where we use equation (2) to fit the data, and we thus find a characteristic grain temperature, which, from equation (3), we can translate into a distance from the star. Using the values of $T_{\rm ex}$ and L_* given in Table 1, we find values for the inner boundary of the dust of 48, 11, 52, and 54 AU around HR 333, HR 506, HR 1082, and HR 3927, respectively. Consistent with models for those dust debris systems where frequent collisions lead to smaller particles that are then ejected by radiation pressure, the stars with the strongest evidence for inner holes in the dust distribution have the highest values of L_{30}/L_*. If the inner holes are caused by inner planets, then in the future, with sufficiently high angular resolution, it may be possible to identify azimuthal asymmetries in the dust that might indicate gravitational perturbations by this unseen system of planets (e.g., Wyatt 2003).

We can also use our data to make a rough estimate of the minimum mass of the parent bodies, $M_{\rm PB}$. Since the Poynting-Robertson drag provides a maximum grain lifetime, then in an approximate steady state we can write (Chen & Jura 2001)

$$M_{\rm PB} \geq \frac{4 L_{30} t_*}{c^2}. \quad (4)$$

This estimate of $M_{\rm PB}$ is insensitive to the grain size and composition; the minimum values of $M_{\rm PB}$ derived from equation (4) are shown in Table 1. In systems with $L_{30}/L_* \gg 10^{-4}$, collisions among dust grains occur often, the Poynting-Robertson lifetime is thus much longer than the collision time, and we may severely underestimate $M_{\rm PB}$. There may also be large objects such as planets that are not experiencing rapid collisions and that do not contribute to the detected dust.

4. DISCUSSION

We show in Table 1 that the inferred lower bounds to $M_{\rm PB}$ range from 0.004 to 0.06 $M_\oplus$. The summed mass of the KBOs in the solar system is uncertain and is currently estimated to be between 0.02 and 0.1 $M_\oplus$ (Bernstein et al. 2004; Luu & Jewitt 2002). Typical analogs of the Kuiper Belt may have total masses $\leq$0.1 $M_\oplus$ (Jura 2004). Since we observed stars with notable infrared excesses, we probably selected objects with particularly massive systems of parent bodies. In the solar system, the value of the infrared luminosity of the dust is $\sim 10^{-7}$ $L_\odot$ (e.g., Fixsen & Dwek 2002). Either the mass of parent bodies around our sample of stars is much larger than the inferred minimum, or the collision rate of these objects is substantially greater than in the Kuiper Belt of the solar system.

Two of the stars in Table 1, λ Boo itself and HR 1570, are λ Boo stars, a subclass of $\sim$2% of all main-sequence A-type stars that is defined as having nearly solar abundances of C, N, and O, but marked deficiencies of Fe elements by factors of 10–100 (Paunzen et al. 2002). The explanation for this abundance pattern is not known. One theory to account for their surface abundances is that they have preferentially accreted some circumstellar matter (Venn & Lambert 1990), and within the star's atmosphere there is an element-dependent chemical separation controlled by gravitational settling and radiative acceleration at the base of the thin outer convection zone of the star (Turcotte & Charbonneau 1993). As shown in Jura (2004), the rate at which circumstellar dust is being produced scales as the infrared excess luminosity such that $\dot{M} \sim L_{30}/c^2$, where c is the speed of light. We therefore find from the results in Table 1 that $\dot{M} \sim 10^{10}$ g s^{-1} for both λ Boo and HR 1570. According to Turcotte & Charbonneau (1993), hydrogen-rich gas infall rates of $\geq 10^{12}$ g s^{-1} with selective accretion of $\geq 10^{10}$ g s^{-1} of metals in dust is required to explain the surface abundances of λ Boo stars. While more sophisticated treatments are required to the accretion/diffusion models, our results at least show that metal infall at the required rate appears to be occurring around λ Boo stars.

In models for the first 100 Myr of the solar system, Petit et al. (2001) have computed that approximately 50% of the $\sim$5 $M_\oplus$ of planetesimals initially within the asteroid belt had their orbits perturbed by Jupiter so they hit the Sun. Murray et al. (2001) have argued that such models can be generally extended to other main-sequence stars. Assuming that this accretion of $\sim 5 \times 10^{12}$ g s^{-1} of rocky material often occurs, the atmospheres of the A stars should be substantially polluted. We speculate that the main-sequence stars with inner holes in their dust distributions may also be systems with asteroidal belts where gravitational perturbations by giant planets lead to a significant supply of metals to an atmosphere where they would otherwise be depleted. An infall of large rocks or asteroids may lead to observable variations in the abundance of the elements in the star's atmosphere (Cowley 1977), which could be different from the effects of dust inflows occurring around the λ Boo stars.

5. CONCLUSIONS

We have obtained *Spitzer* mid-infrared spectra of 19 main-sequence stars. Our data are most useful for constraining the evolution of the solid material in regions between $\sim$10 and $\sim$60 AU from the stars. We conclude the following.

1. There are no strong spectral features; we suggest that the typical diameter of a dust particle is greater than 10 μm.

2. The infrared excesses can be explained by dust arising from collisions between parent bodies whose minimum total mass lies between 0.004 and 0.06 $M_\oplus$. These derived minimum masses are comparable to the total mass of KBOs in the solar system.

3. We estimate dust production rates of $\sim 10^{10}$ g s^{-1} around λ Boo and HR 1570; selective accretion of this material may help explain their peculiar surface abundances.

4. There appear to be inner truncations in the dust clouds at 48, 11, 52, and 54 AU around HR 333, HR 506, HR 1082, and HR 3927, respectively.

This work is based on observations made with the *Spitzer* Space Telescope, which is operated by the Jet Propulsion Laboratory, California Institute of Technology, under NASA contract 1407. Support for this work was provided by NASA through Contract Number 1257184 issued by JPL/Caltech. F. K. is supported by the *Spitzer* Fellowship Program under award 011 808-001. Work at Cornell and the University of Rochester has been supported by JPL contract 960803 to Cornell and Cornell subcontract 31419-5714 to the University of Rochester. We are grateful to the entire team of scientists and engineers who have made *Spitzer* and the IRS function so well.

REFERENCES

Aumann, H. H., et al. 1984, ApJ, 278, L23
Bernstein, G. M., Trilling, D. E., Allen, R. L., Brown, M. E., Holman, M., & Malhorta, R. 2004, AJ, in press
Buitrago, J., & Mediavilla, E. 1985, A&A, 148, L8
Chen, C. H., & Jura, M. 2001, ApJ, 560, L171
Cohen, M., Megeath, T. G., Hammersley, P. L., Martin-Lui, F., & Stauffer, J. 2003, AJ, 125, 2645
Cowley, C. 1977, Ap&SS, 51, 349
Decin, G., Dominik, C., Malfait, K., Mayor, M., & Waelkens, C. 2000, A&A, 357, 533
Decin, G., Dominik, C., Waters, L. B. F. M., & Waelkens, C. 2003, ApJ, 598, 636
Fixsen, D. J., & Dwek, E. 2002, ApJ, 578, 1009
Flower, P. J. 1996, ApJ, 469, 355
Habing, H. J., et al. 2001, A&A, 365, 545
Heiter, U., Weiss, W. W., & Paunzen, E. 2002, A&A, 381, 971
Higdon, S. J. U. 2004, PASP, submitted
Houck, J., et al. 2004, ApJS, 154, 18
Israelian, G., Santos, N. C., Mayor, M., & Rebolo, R. 2004, A&A, 414, 601
Jura, M. 2004, ApJ, 603, 729
Jura, M., Malkan, M., White, R., Telesco, C., Pina, R., & Fisher, R. S. 1998, ApJ, 505, 897
Kenyon, S. J., & Bromley, B. C. 2002, ApJ, 577, L35
Krivov, A. V., Mann, I., & Krivova, N. A. 2000, A&A, 362, 1127
Lagrange, A.-M., Backman, D. E., & Artymowicz, P. 2000, in Protostars and Planets IV, ed. V. Mannings, A. Boss, & S. S. Russell (Tucson: Univ. Arizona Press), 639
Luu, J. X., & Jewitt, D. C. 2002, ARA&A, 40, 63
Murray, N., Chaboyer, B., Arras, P., Hansen, B., & Noyes, R. W. 2001, ApJ, 555, 801
Paunzen, E., Iliev, I. Kh., Kamp, I., & Barzova, S. 2002, MNRAS, 336, 1030
Petit, J.-M., Morbidelli, A., & Chambers, J. 2001, Icarus, 153, 338
Schneider, G., et al. 1999, ApJ, 513, L127
Song, I., Caillault, J.-P., Barrado y Navascues, D., & Stauffer, J. R. 2001, ApJ, 546, 352
Spangler, C., Sargent, A. I., Silverstone, M. D., Becklin, E. E., & Zuckerman, B. 2001, ApJ, 555, 932
Spitzer, L. 1978, Physical Processes in the Interstellar Medium (New York: Wiley Interscience)
Takeuchi, T., & Artymowicz, P. 2001, ApJ, 557, 990
Turcotte, S., & Charbonneau, P. 1993, ApJ, 413, 376
Venn, K. A., & Lambert, D. L. 1990, ApJ, 363, 234
Werner, M. W., et al. 2004, ApJS, 154, 1
Wolf, S., & Hillenbrand, L. A. 2003, ApJ, 596, 603
Wyatt, M. C. 2003, ApJ, 598, 1321
Wyatt, M. C., & Dent, W. R. F. 2002, MNRAS, 334, 589
Zuckerman, B. 2001, ARA&A, 39, 549
Zuckerman, B., & Song, I. 2004, ApJ, 603, 738

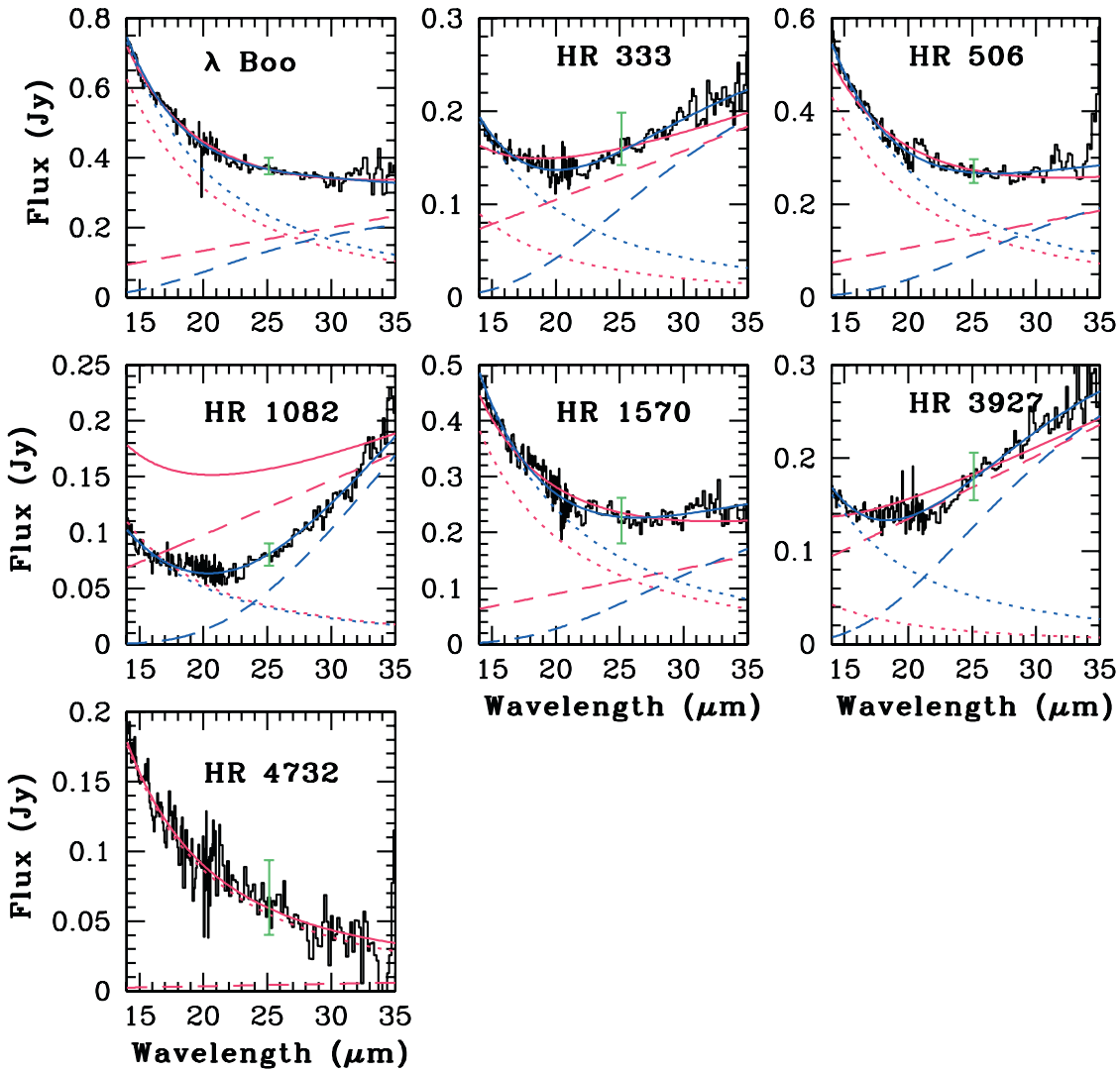

FIG. 1.—Plots of F_ν vs. λ for the six stars in Table 1 plus HR 4732, which has, at most, a modest infrared excess. The fits from eq. (1) are shown in red, while the fits from eq. (2) are shown in blue. We also display 3 σ error bars at 25 μm in green. The sum of the two terms in each equation is given by a solid line, while dotted and dashed lines represent the photospheric fluxes and dust excesses, respectively.